Renewable and Sustainable Energy Reviews 33 (2014) 382–391

Contents lists available at ScienceDirect

Renewable and Sustainable Energy Reviews

journal homepage: www.elsevier.com/locate/rser

Assessment of the global ocean wind energy resource

Chong wei Zheng [a,b,c,*], Jing Pan [b]

[a] College of Meteorology and Oceanography, People's Liberation Army University of Science & Technology, Nanjing 211101, China
[b] National Key Laboratory of Numerical Modeling for Atmospheric Sciences and Geophysical Fluid Dynamics (LASG), Institute of Atmospheric Physics, Chinese Academy of Sciences, Beijing 100029, China
[c] No. 92538 of People's Liberation Army, Dalian 116041, China

ARTICLE INFO

Article history:
Received 25 October 2012
Received in revised form
13 December 2013
Accepted 27 January 2014
Available online 4 March 2014

Keywords:
Global ocean
Wind energy resource
CCMP wind field data
Wind energy storage
Long-term trend
Grade classification map

ABSTRACT

Against a background of an environmental and resources crisis, the exploitation of renewable and clean energy can effectively alleviate the energy crisis and contribute to emission reduction and environmental protection, thus promoting sustainable development. This study aims to develop a grade classification map of the global ocean wind energy resource based on CCMP (cross-calibrated, multi-platform) wind field data for the period 1988–2011. We also calculate, for the first time, the total storage and effective storage of wind energy across the global ocean on a $0.25^\circ \times 0.25^\circ$ grid. An optimistic increasing long-term trend in wind power density was found. In addition, the global ocean wind energy resource was analyzed and regionalized by considering the temporal and spatial distributions of wind power density, wind energy levels, and effective wind speed, as well as through a consideration of wind energy storage and the stability and long-term trends of wind power density. This research fills a gap in our knowledge in this field, and provides a reference point for future scientific research and development into wind energy resources such as wind power generation, water pumping, and wind-heating.

Contents

1. Introduction . . . 382
2. Wind field data . . . 383
3. Assessment of the global ocean wind-energy resource . . . 384
   3.1. Seasonal characteristics of wind power density . . . 384
   3.2. Distribution of energy level occurrence . . . 384
   3.3. Occurrence of effective wind speed . . . 385
   3.4. Stability of wind power density . . . 386
      3.4.1. Coefficient of variation . . . 387
      3.4.2. Monthly variability index . . . 387
      3.4.3. Seasonal variability index . . . 387
   3.5. Storage of wind energy . . . 388
   3.6. Long-term trend in wind power density . . . 388
   3.7. Classification of global ocean wind energy resource . . . 388
4. Conclusions . . . 390
Acknowledgments . . . 391
References . . . 391

1. Introduction

Against a background of an environmental and resources crisis, the ongoing development of clean energy sources seems increasingly inevitable if we are to deal with climate change and the

* Corresponding author at: Meteorological station, No. 1 Chaohai Street, Lvshunkou District of Dalian City, Dalian 116041, China. Tel.: +86 18640814027; fax: +86 041185883108.
E-mail address: chinaoceanzcw@sina.cn (C.w. Zheng).

http://dx.doi.org/10.1016/j.rser.2014.01.065
1364-0321

Nomenclature

ADEOS-II	advanced earth observing satellite, 2nd generation
AMSR-E	advanced microwave scanning radiometer-earth observing system
CCMP	Cross-calibrated, multi-platform
C_v	coefficient of variation
DOE	Department of Energy of the United States
ECMWF	European Centre for Medium-Range Weather Forecasts
ECOP	ECMWF operational
ERA-40	40-year ECMWF re-analysis
MAM	March, April, and May
M_v	monthly variability index
PO.DAAC	Physical Oceanography Distributed Active Archive Center
RSS	remote sensing systems
SSM/I	special sensor microwave imager
S_v	seasonal variability index
TC-114	Technical Committee 114
TMI	tropical rainfall measuring mission microwave imager
VAM	variational analysis method
WW3	WAVEWATCH-III

energy crisis [1,2]. Currently, the utilization of solar and on-land wind energy is trending towards industrialization, although both are restricted by geographical factors. Despite nuclear power generation being an effective energy source, it is also vulnerable to natural disasters and human error. For example, both the nuclear leakage caused by the tsunami in January 2011 in Japan, and the Chernobyl nuclear disaster caused by operator errors in 1986, resulted in extremely serious consequences. Offshore wind energy offers substantial advantages over land-based turbines, including resource storage and greater stability [3–6]. Electivity generation by wind power is the principal mode of wind energy resource development, but wind power also has wide applications within navigation, water pumping, wind-heating, etc. However, offshore wind power generation can provide the solutions of most practical value and so meet urgent demands associated with problems such as coastal cities with a high demand for electricity, thereby closing the huge energy gap, and can serve remote islands, lighthouses at sea, marine weather buoys, and other power supply scenarios in marine areas. This largely impeded the economic leap of the coastal city and rural island, meanwhile this predicament promises offshore wind power with broad prospects. Consequently, the promise of abundant wind energy has become a particular area of interest for developed countries [7,8].

The distribution of wind energy resource shows significant regional and seasonal differences, and in the large-scale development of wind power, the basic principle is one of 'resource evaluation and planning ahead'. Blanco [9] calculated the onshore and offshore wind energy cost in Europe and pointed out that the local wind resource is by far the most important factor affecting the profitability of wind energy investments. An on-land wind energy distribution map of the United State was drawn up in 1986 using observations from 1000 weather stations [10]. The Risoe National Laboratory in Denmark collected observational data from 220 stations in 12 European countries, and then developed an on-land wind-energy distribution map for Europe [11]. Previous researchers have made great contributions to the assessment of the potential of wind energy, but due to the lack of offshore wind data, most previous studies have focused on land, coastal, or local sea sites, rather than the global ocean wind-energy resource. In 1994, Gaudiosi [12] presented the characteristics of offshore wind-energy activity for the Mediterranean and other European seas. Emphasis was given to wind resource assessment, technical development, applications, economics, and environment. To promote wind energy in Senegal, Youm et al. [13] analyzed the wind energy potential along its northern coast, using wind data collected over a period of 2 years at five different locations. With an annual mean wind speed of 3.8 m/s, an annual energy of 158 kWh/m^2 could be extracted. Results show that a potential use of wind energy in these locations is water pumping in rural areas. Karamanis [14] analyzed the wind energy resources on the Ionian–Adriatic coast of southeast Europe and showed that the mean wind-power densities were less than 200 W/m^2 at 10 m height, suggesting the limited suitability of these sites for the usual wind-energy applications. However, these results indicate that wind power plants, even in lower-resource areas, can be competitive in terms of the energy payback period and reducing greenhouse emissions. With the rapid development of ocean observation technology, increasing amounts of satellite wind data have been used to analyze wind-energy resources. In 2008, NASA [15] and Liu et al. [16] contoured global wind-power density in JJA (June, July, and August) and DJF (December, January, and February), using QuikSCAT wind data. They found that the wind power density in the winter hemisphere is significantly higher than that in the summer hemisphere. During JJA, the regions of highest wind power density are located mainly around the Southern Hemisphere westerlies (ca. 1000–1400 W/m^2) and the waters surrounding Somalia (ca. 1200 W/m^2). During DJF, the areas of highest wind power density are located mainly around the Northern Hemisphere westerlies (ca. 1000–1400 W/m^2). Obviously, the wind power around the Southern Hemisphere westerlies during DJF is less than that during JJA.

However, until now, there has been no comprehensive assessment of the distribution of the grade (see Table 1) of global ocean wind energy resources. This study presents a grade classification map of the global ocean wind energy resource based on CCMP (cross-calibrated, multi-platform) wind field data for the period 1988–2011, and also calculates, for the first time, the total storage and effective storage of wind energy across the global ocean (on a $0.25^\circ \times 0.25^\circ$ grid). Synthetically considering the wind power density, the distribution of wind energy levels and effective wind speeds, the stability and long-term trend of wind power density, and wind energy storage, we were able to analyze and regionalize the global ocean wind energy resource. The aim of this research is to fill the gap in our understanding in this field and provide guidance for future scientific research and development into wind energy resources such as electricity generation, water pumping, and wind-heating. We also hope to make a contribution towards alleviating the energy crisis and promoting sustainable development.

2. Wind field data

The CCMP wind field data are hosted at the Physical Oceanography Distributed Active Archive Center (PO.DAAC) and have been evaluated and utilized extensively by the scientific community [17]. The data are derived through the cross-calibration and assimilation of ocean surface wind data from SSM/I (Special Sensor Microwave Imager), TMI (Tropical Rainfall Measuring Mission Microwave Imager), AMSR-E (Advanced Microwave Scanning Radiometer-Earth Observing System), SeaWinds on QuikSCAT, and SeaWinds on ADEOS-II (Advanced Earth

Table 1
Standard of wind power classification [24–27].

Wind power class	Annual average wind speed (m/s)	Annual average wind power density (W/m^2)		Significant interval (h)	Wind energy division
		Method 1	Method 2		
1	0.0–4.4	<100	<50	<2000	Indigent area
2	4.4–5.1	100–150	50–150	2000–3000	Available area
3	5.1–5.6	150–200	150–200	3000–5000	Subrich area
4	5.6–6.0	200–250	200–250	>5000	Rich area
5	6.0–6.4	250–300	250–300		
6	6.4–7.0	300–400	300–400		
7	7.0–9.4	400–1000	400–1000		

Observing Satellite, 2nd Generation). Cross-calibration is performed by Remote Sensing Systems (RSS) under the DISCOVER project. These datasets are combined with conventional observations and a starting estimate of the wind field using a variational analysis method (VAM). The VAM requires a background (or first guess) analysis of gridded u and v wind components as a prior estimate of the wind field. The 40-year ECMWF (European Centre for Medium-Range Weather Forecasts) Re-Analysis (ERA-40) was used as the background for the period July 1987–December 1998. Beginning in 1999, with the benefits of 4D variational data assimilation (4DVAR) and increased spatial resolution, the ECMWF operational (ECOP) analysis outperforms the ERA-40 and is used here for the background. For ECOP, the temporal resolution is 6 h, the spatial resolution is $0.25^\circ \times 0.25^\circ$, the period covered is July 1987–December 2011, and the area covered is 78.375°S–78.375°N, 180°W–180°E.

3. Assessment of the global ocean wind-energy resource

Wind power density was calculated as follows:

$$W = \frac{1}{2}\rho V^3 \tag{1}$$

where W is the wind power density (W/m^2), V is the sea surface wind speed (m/s), and p is the standard sea-level air density (1.225 kg/m^2) [18–20]. By combining expression (1) with the CCMP wind field data, we obtained the 6-hourly global ocean wind power density of 10 m above the sea surface for the period 1988–2011.

3.1. Seasonal characteristics of wind power density

Wind power density exhibits obvious seasonal and regional differences across the global ocean. Here, only the wind power density during JJA (June, July, and August) and DJF (December, January, and February), as well as the annual average, are shown (Fig. 1).

As shown in Fig. 1, the wind power density in the winter hemisphere is considerably larger than that in the summer hemisphere, and also exhibits significant regional differences. Under the influence of strong westerly winds, large areas of wind power density are distributed mainly around the Northern and Southern Hemisphere westerlies, with the maximum appearing under the ‘roaring westerlies’. The distribution of global ocean wind-power density is consistent with the conclusions of NASA [15] and Liu et al. [16].

Regarding the annual average value, the areas of highest wind power density are distributed mainly around the Southern Hemisphere westerlies (800–1600 W/m^2) and the Northern Hemisphere westerlies (600–1000 W/m^2). Influenced by the southwest monsoon during JJA, the coast of Somalia shows a relatively large area of >400 W/m^2 in wind power density. Affected by the northeast monsoon during DJF, the waters surrounding Taiwan also show as a relatively large area of >400 W/m^2 in wind power density. Wind power density in the middle- and low-latitude waters is 200–400 W/m^2, while for most of the equatorial waters it is <200 W/m^2. Dong et al. [21] analyzed the offshore wind energy resources of the coastal areas of Shandong Province, and reported that the annual average wind speed in this region is above 6.0 m/s, and that wind power density can reach 225 W/m^2 or higher. Our result of wind power density in the coastal areas of Shandong Province (about 200 W/m^2) is slightly less than that reported by Dong et al. [21], and our result is also consistent with the findings of Karamanis [14] from the west coast of Greece (<200 W/m^2 at 10 m).

3.2. Distribution of energy level occurrence

In the exploitation of wind energy resource, energy level occurrence is one of the important factors used to quantify the richness of the wind energy. Usually, wind power can be utilized when the wind power density is above 50 W/m^2, and areas with power densities above 200 W/m^2 can be classified as energy-rich regions [3–4]. In this study, we statistics the occurrence of wind power density greater than 50 W/m^2, and also where it was greater than 200 W/m^2 during MAM (March, April, and May), JJA, SON (September, October, and November), and DJF; we also calculated the annual occurrence. Here, only the annual occurrence over the past 24 years is shown (Fig. 2).

A wind power density of greater than 50 W/m^2 occurs for 80% of the year over most of the global ocean (Fig. 2a). Only at the poles and isolated spots scattered along the equator is the frequency of occurrence relatively low, but it still exceeds 50% of the year.

The seasonal distribution of wind power density levels greater than 200 W/m^2 (figure not shown) shows that during MAM, the high occurrence areas are distributed mainly around the Northern and Southern Hemisphere westerlies, the North Pacific mid–low latitude waters (at approximately 10°N and showing a west–east zonal distribution), low latitudes in the North Atlantic, mid-latitudes in the southern Indian Ocean (around 25°S, zonal distribution), the South Pacific eastern mid-latitude waters (around 20°S–25°S, 120°W–70°W), and mid-latitudes in the South Atlantic, while the low-frequency areas were mainly located near the poles and the equator. During JJA, it is summer in the Northern Hemisphere, so the occurrence is lower than that in the Southern Hemisphere overall, and the Southern Hemisphere westerlies and the Arabian Sea can reach 80% or higher at this time. The occurrence during SON is similar to that in MAM, although slightly higher. During DJF, the high occurrence areas are distributed around the Northern and Southern Hemisphere westerlies, the China Sea, the North Pacific Ocean mid- to low-latitude waters,

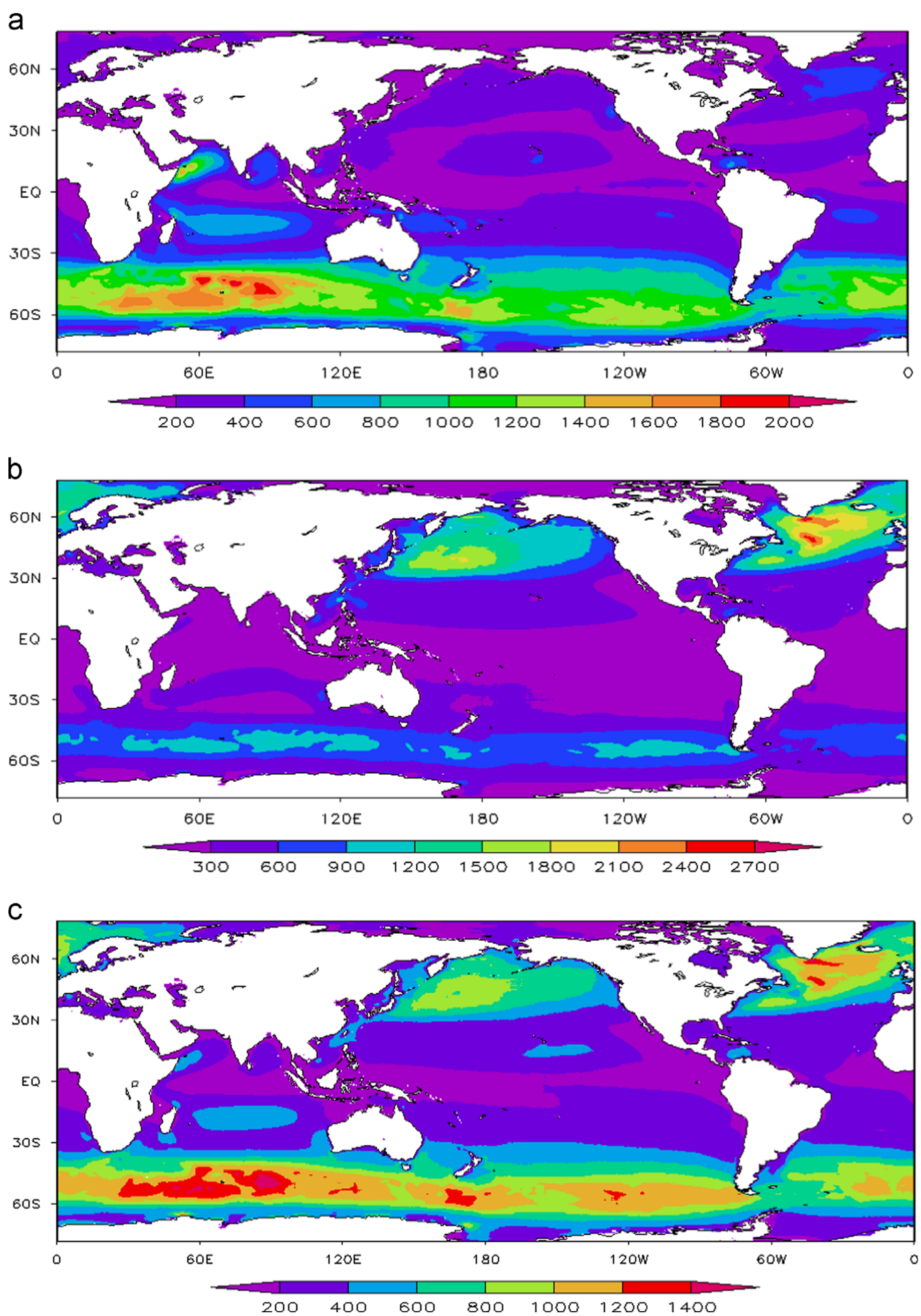


Fig. 1. Wind power density during (a) JJA, (b) DJF, and (c) the annual average over the past 24 years (units: W/m^2).

low latitudes in the North Atlantic, and the coast of Somalia. Low occurrence waters are mainly distributed around the poles and equator.

Areas where the wind power density has commonly exceeded 200 W/m^2 over the past 24 years (Fig. 2b) are mainly located around the Northern Hemisphere and Southern Hemisphere westerlies, the Northern Hemisphere near 10°N, and around 20°S in the Southern Hemisphere. Low occurrence waters are seen at the poles, in the central and eastern equatorial Indian Ocean, the western equatorial Pacific, in the nearshore zone of the eastern equatorial Pacific, and the equatorial Atlantic in mid-eastern waters.

3.3. *Occurrence of effective wind speed*

Effective wind speed means that the wind speed is suitable for the development of wind energy resources, and it is defined as 5–25 m/s [22]. Using 6-hourly wind speed data from the period 1988–2011, we calculated the occurrence of effective wind speed during MAM, JJA, SON, DJF and annually. Here, only the annual occurrence for the past 24 years is shown (Fig. 3).

Whether during MAM, JJA, SON, or DJF, the occurrence of effective wind speed across the global oceans is high overall; i.e., above 60% year-round, except for some small areas near the equator and some coastal waters, and this is of benefit for the

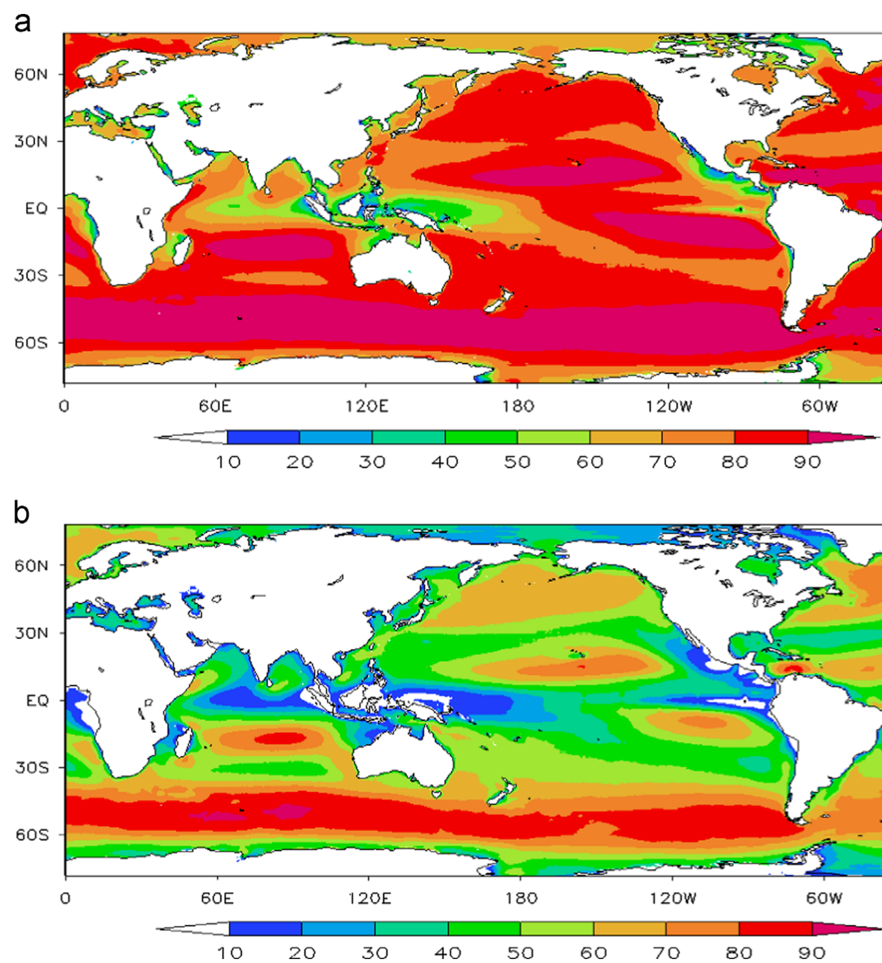


Fig. 2. Annual occurrence of wind power density greater than (a) 50 W/m^2 and (b) 200 W/m^2 (units: %).

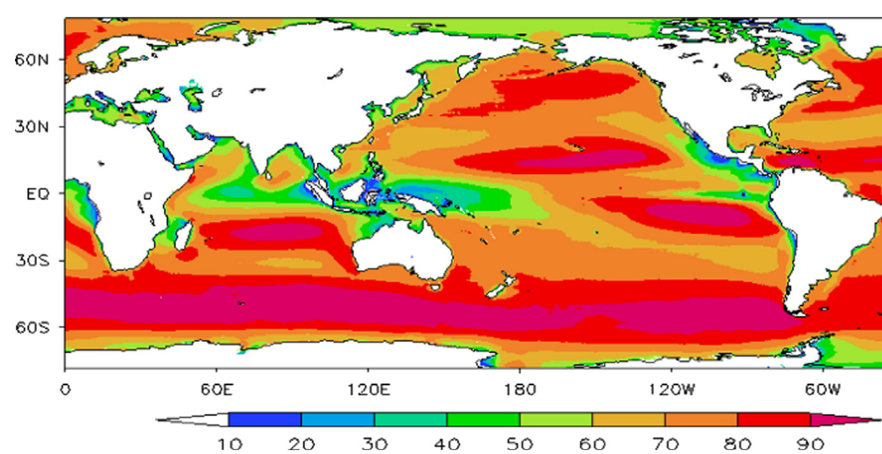


Fig. 3. Annual occurrence of effective wind speed over the past 24 years (units: %).

development of wind energy resources. Considering the annual occurrence over the past 24 years (Fig. 3), the large areas of consistently high effective wind speeds are distributed mainly around the Southern Hemisphere westerlies (> 80%), the Northern Hemisphere westerlies (> 70%), the Northern Hemisphere near 10°N (ca. 80%), and around 20°S in the Southern Hemisphere (ca. 80–90%), while the low-occurrence areas are located mainly near the poles, the central and eastern equatorial Indian Ocean, the western equatorial Pacific, the nearshore zone of the eastern equatorial Pacific, and the eastern equatorial Atlantic.

3.4. Stability of wind power density

During the development of ocean energy resources, it is necessary to consider energy stability [23]. A stable wind power density is beneficial to the gatheration and conversion of wind energy. Unstable wind power density not only lowers conversion efficiency, but might also damage the generating equipment. Stability can be assessed using the statistics C_v (coefficient of variation), M_v (monthly variability index), and S_v (seasonal variability index) obtained from the wind power density data.

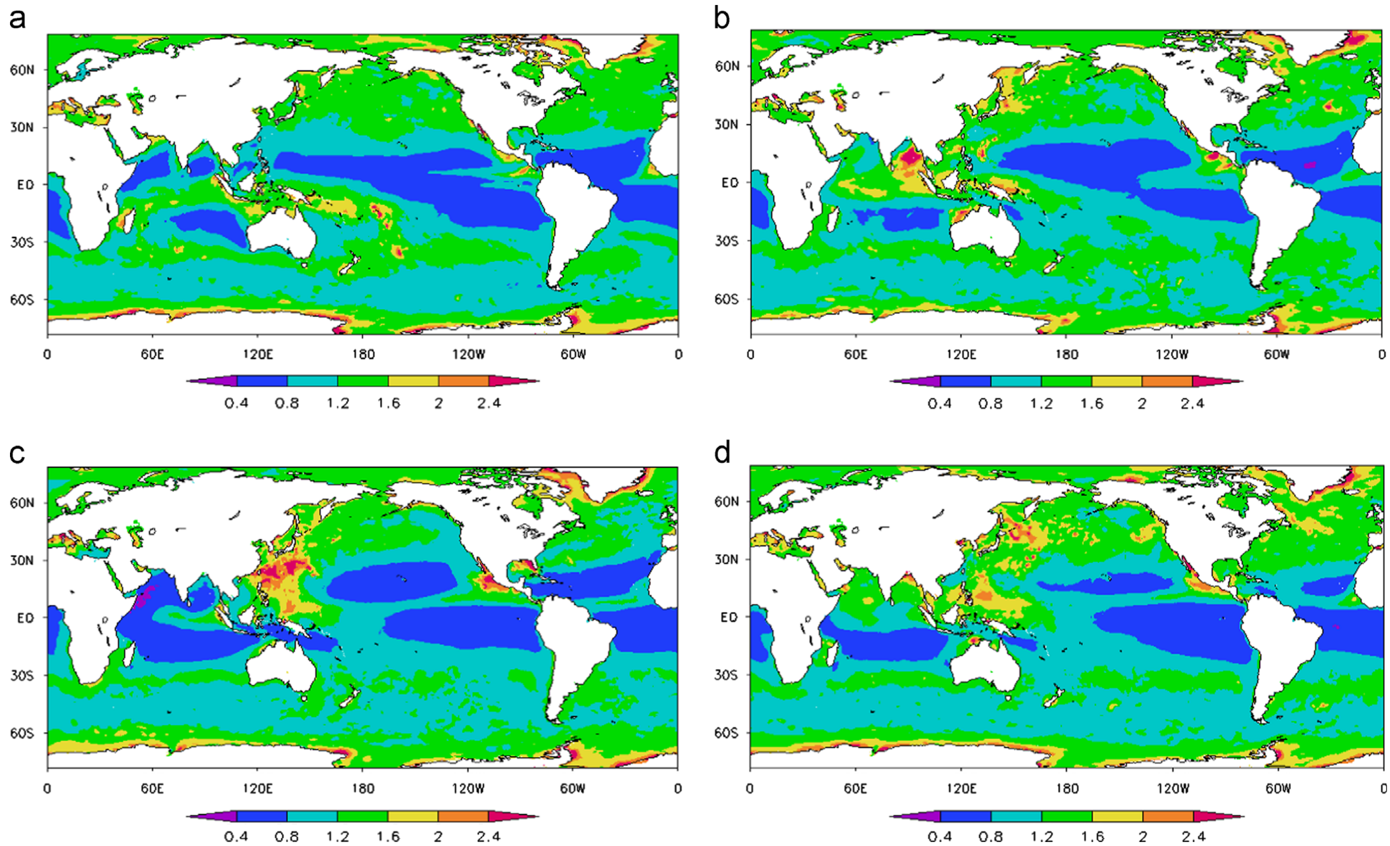


Fig. 4. Coefficient of variation of wind power density in (a) January, (b) April, (c) July, and (d) October across the global ocean over the past 24 years.

3.4.1. *Coefficient of variation*

The smaller the C_v, the greater the stability of the energy density, and this is calculated as follows:

$$C_v = \frac{S}{\bar{x}}, \tag{2}$$

where C_v is the coefficient of variation, as shown in Fig. 4. $\bar{x}$ is the mean value, and S is the standard deviation, calculated as follows:

$$S = \frac{\sqrt{\sum_{i=1}^{n} x_i^2 - \left(\sum_{i=1}^{n} x_i\right)^2 / n}}{n-1} \tag{3}$$

where n is the number of data points.

Regarding the seasonal differences, the C_v during DJF (January as the representative month) is significantly better than in MAM (April as the representative month), JJA (July as the representative month), and SON (October as the representative month). There are several perennial areas of higher stability: the North Pacific near the equator, the eastern low latitudes of the South Pacific, the low-latitude waters of the Atlantic Ocean, the northern Indian Ocean near the equator, and the southern Indian Ocean at low latitudes, all with a C_v below 0.8 all year round.

Regarding the regional differences, the C_v in the Southern Ocean is better (lower) than that in the Northern Ocean, and the stability is also better offshore than nearshore, in the middle- and low-latitude waters than in the high-latitude waters, and on eastern coasts than western coasts. The lowest stability was found at the poles.

3.4.2. *Monthly variability index*

The greater the M_v, the monthly variation of energy density, the worse is the monthly stability. M_v is calculated as follows:

$$M_v = \frac{P_{M1} - P_{M12}}{P_{year}} \tag{4}$$

where P_{M1} is the month with the highest energy density, P_{M12} is the month with the lowest energy density, and P_{year} is the annual average energy density (Fig. 5).

The M_v index of wind power density across most of the global ocean is below 4.0, which means that wind power density in most areas does not show strong monthly variations. However, the M_v index does show obvious regional differences: the M_v index in the Southern Hemisphere as a whole is lower than that in the Northern Hemisphere, which indicates that the monthly stability of wind power density in the Southern Ocean is better than that in the Northern Ocean. The M_v index in the coastal waters of the Northern Hemisphere is higher than that in the offshore areas. Lower monthly stability is seen in the Arabian Sea, western equatorial Pacific, and around the North Pacific and North Atlantic westerlies, as well as in most of the coastal waters of the Northern Hemisphere, with the M_v index even rising above 6.0 in some places.

3.4.3. *Seasonal variability index*

The greater the S_v, the seasonal variation of energy density, the poorer the seasonal stability. S_v is calculated as follows:

$$S_v = \frac{P_{S1} - P_{S4}}{P_{year}} \tag{5}$$

where P_{S1} is the season with the highest energy density, P_{S4} is the season with the lowest energy density, and P_{year} is the annual average energy density (Fig. 6).

Overall, the distribution pattern of the S_v index is similar to that of the M_v index, although it is numerically lower than M_v, as shown in Figs. 5 and 6.

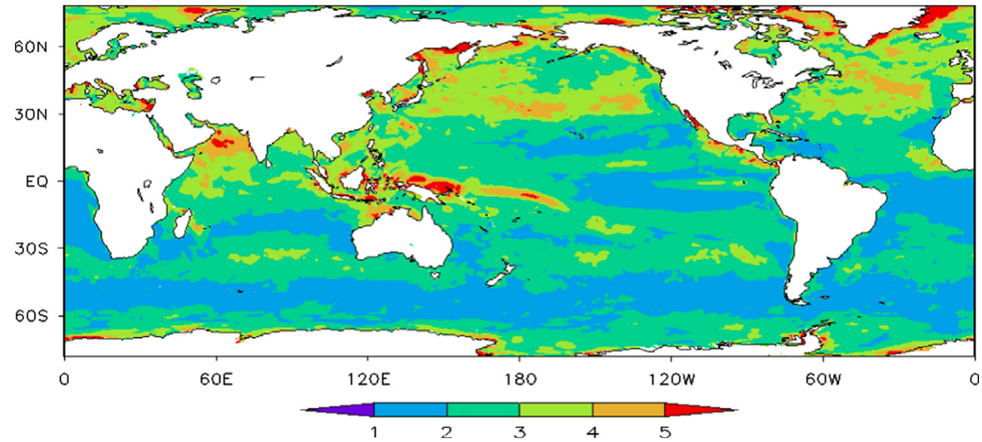


Fig. 5. Distribution of monthly variability index of wind power density across the global ocean.

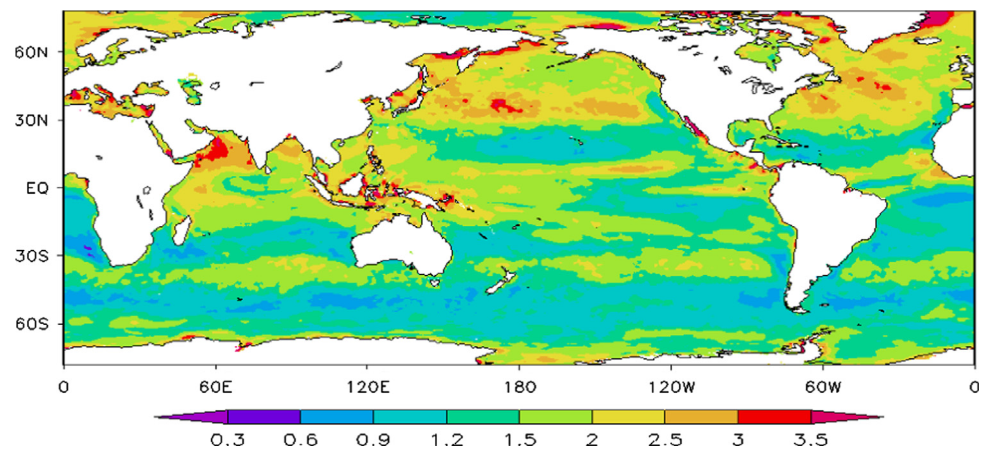


Fig. 6. Distribution of the seasonal variability index of wind power density across the global ocean.

3.5. Storage of wind energy

To analyze the storage of wind energy in detail, we calculated the per unit area total storage, effective storage, and exploitable storage of global ocean wind energy using a $0.25^\circ \times 0.25^\circ$ grid (Fig. 7) and the calculation method below:

$$E_{PT} = \overline{P}*H \tag{6}$$

$$E_{PE} = \overline{P}*H_E \tag{7}$$

$$E_{PD} = E_{PE}*C_e \tag{8}$$

where E_{PT} is the total storage of wind energy, $\overline{P}$ is the annual average wind-power density, and H=365d × 24 h=8760 h. In Eq. (7), E_{PE} is the effective storage of wind energy and H_E is the annual total number of hours of effective wind speed. In Eq. (8), E_{PD} is the technological development volume of wind energy resources, and C_e=0.785; i.e., the actual swept area of the wind turbine blades is 0.785, meaning that for a diameter of 1 m, the swept area of the wind turbine is calculated from 0.52 × p, which equals 0.785 m^2.

Fig. 7a shows that the total storage of wind energy resources across most of the global oceans is above 2×10^3 kWh/m^2, but is less near the equator (but still above 1×10^3 kWh/m^2). High-storage areas are concentrated around the westerlies in the Northern and Southern Hemispheres, and storage decreases gradually towards lower latitudes. Total storage around the Southern Hemisphere westerlies is typically greater than 6×10^3 kWh/m^2, and reaches 12×10^3 kWh/m^2 or more in some areas, while 4×10^3 kWh/m^2 is typical for the western North Pacific, with 5×10^3 kWh/m^2 or more around the North Atlantic westerlies.

The distribution pattern of the effective storage of wind energy resources is consistent with the total storage, which may due to the high frequency of effective wind speed across all global oceans. The exploitable storage of wind energy resources is 0.785 times the effective storage.

3.6. Long-term trend in wind power density

We now consider the long-term trend in wind power density over the period 1988–2011 using a $0.25^\circ \times 0.25^\circ$ grid across the global oceans (Fig. 8). For the past 24 years, wind power density has followed a significant increasing trend in most of the global oceans, which is of considerable benefit to wind energy development. Areas with a strong increasing trend are mainly located around the westerlies in the Northern Hemisphere (> 4 W/m^2/year) and Southern Hemisphere (> 8 W/m^2/year), with the increase reaching 20 W/m^2/yr or more in some areas. The increasing trend in mid- to low-latitude waters is less than 5 W/m^2/year. The increasing trend on western coasts is stronger than that on eastern coasts, while only a few scattered locations show no significant trend.

3.7. Classification of global ocean wind energy resource

According to technical standards for wind energy resources development created by the DOE (Department of Energy of the

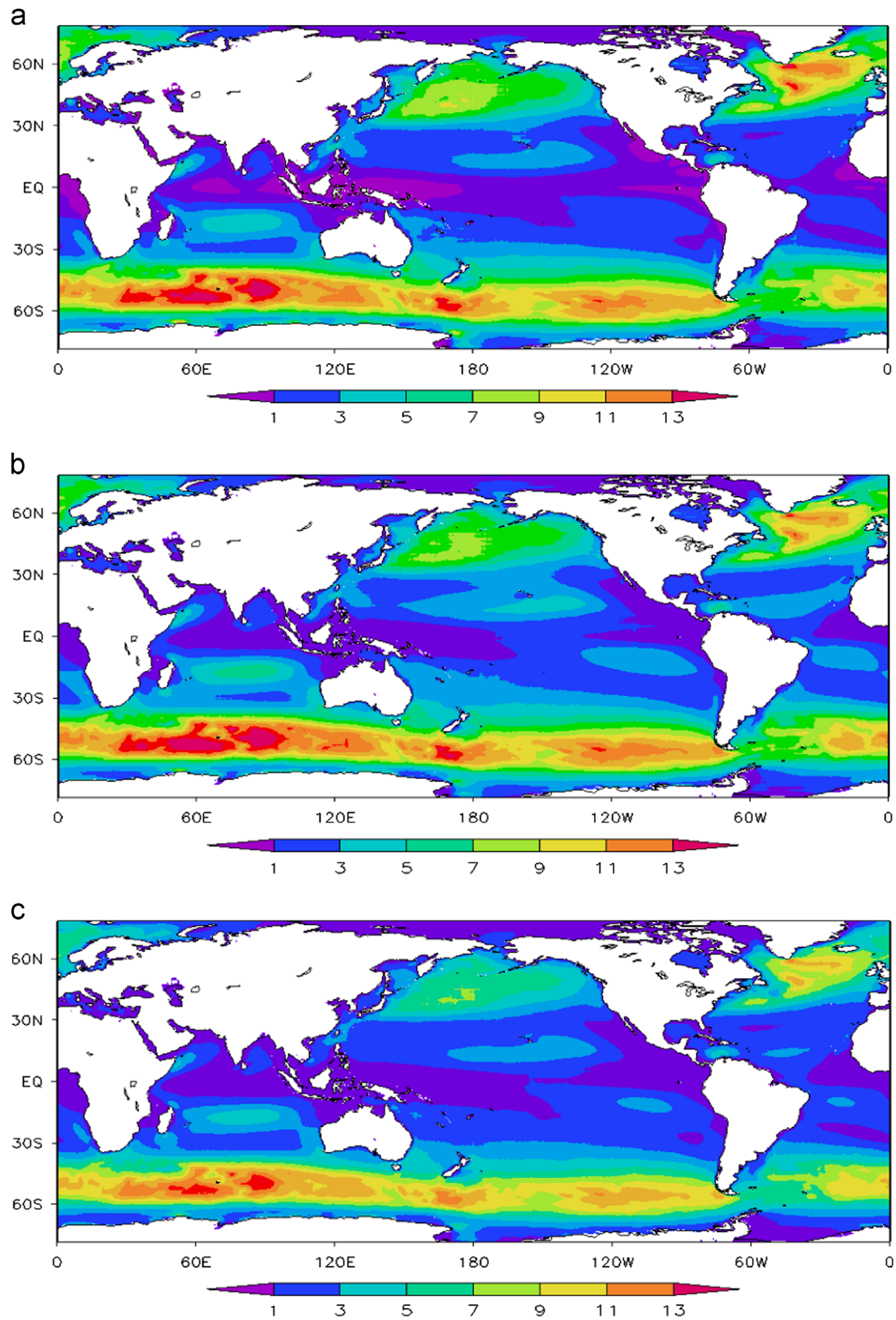


Fig. 7. (a) Total storage, (b) effective storage, and (c) exploitable storage of wind energy resource across the global ocean (units: 10^3 kWh/m^2).

United State) [24,25] and National Development and Reform Commission of China [26,27], wind energy can be classified into indigent area (area not suitable for wind energy development), available area (although not rich region, wind energy development can also be carried out), subrich area (relatively abundant area, which is suitable for wind energy development), and rich area (abundant area, which is very suitable for wind energy development). These classes ranged from Class 1 (the lowest) to Class 7 (the highest), as shown in Table 1.

As part of this study, we created a grade classification map of the global ocean wind energy resource based on the CCMP wind field data for the period 1988–2011 and using the wind energy grading standards of the DOE (Table 1; Fig. 9).

Fig. 9 shows that most of the global oceans are rich in wind energy resources, and especially enriched are the westerly belts of both hemispheres. Indigent areas are mainly scattered around the equator and poles, while available and subrich areas are found in low-latitude waters, the coastal waters of the eastern Pacific Ocean at mid to low latitudes, and most of the waters around the poles.

While the global oceans are rich in wind energy resource, the difficulties associated with electrical power generation and transmission, including shortages of conventional energy, are increasing. The

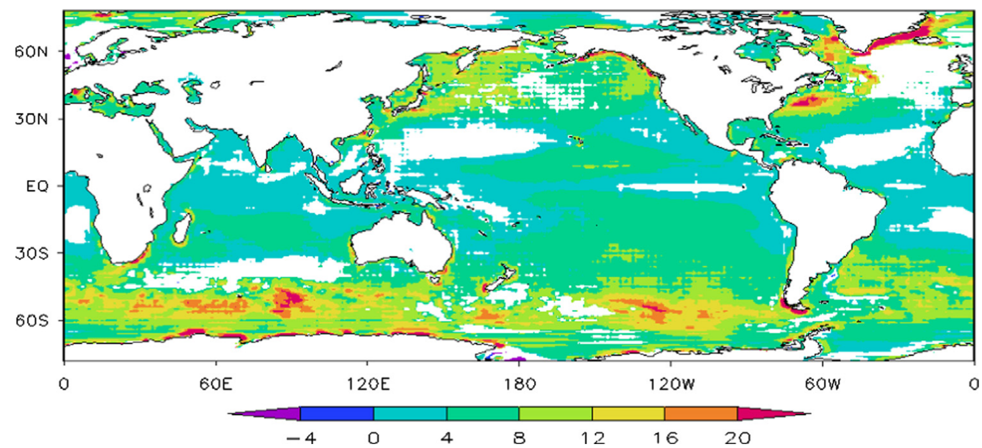


Fig. 8. Long-term trend in wind power density for the period 1988–2011 across the global ocean (units: W/m^2/year). Only trends significant at the 95% level are shown.

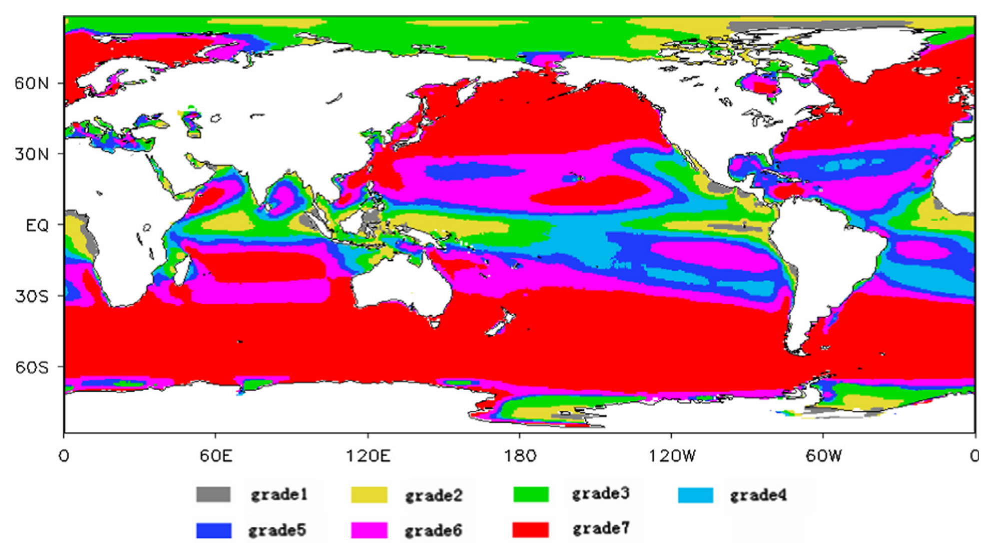


Fig. 9. Grade classification map of the global ocean wind energy resource.

vigorous development of wind energy may offer one approach to tackling these problems.

4. Conclusions

1. The wind power density in the winter hemisphere is significantly larger than that in the summer hemisphere. Large areas of high wind-power density are concentrated around the Southern Hemisphere westerlies (800–1600 W/m^2) and Northern Hemisphere westerlies (600–1000 W/m^2), followed by the coast of Somalia and the waters surrounding Taiwan (> 400 W/m^2). Wind power density in mid- to low-latitude waters is 200–400 W/m^2, while in most of the equatorial waters it is less than 200 W/m^2.
2. A wind power density greater than 50 W/m^2 is available in most of the global oceans for more than 80% of the year. Areas where wind power density commonly exceeds 200 W/m^2 are located around the Northern and Southern Hemisphere westerlies, the Northern Hemisphere near 10°N, and around 20°S in the Southern Hemisphere. Areas of persistently low wind-power density occur around the poles, the central and eastern equatorial Indian Ocean, the western equatorial Pacific, nearshore areas in the eastern equatorial Pacific, and the eastern equatorial Atlantic.
3. The occurrence of effective wind speed is high across the global ocean, above 60% year-round, except for some small areas near the equator and some coastal waters. This phenomenon is of benefit for the development of wind energy resource. Areas of high effective wind speed are found around the Southern Hemisphere westerlies (> 80%), the Northern Hemisphere westerlies (> 70%), the Northern Hemisphere near 10°N (ca. 80%), and around 20°S in the Southern Hemisphere (ca. 80% to 90%).
4. The stability of wind power density in the Southern Ocean is better than that in the Northern Ocean, it is also better in offshore than nearshore areas, in mid- to low-latitude waters than in high-latitude waters, and on eastern coasts than western coasts. The lowest stability occurs at the poles, as demonstrated by the distributions of the coefficient of variation, monthly variability index, and seasonal variability index.
5. The total storage of wind energy resources across most of the global oceans is above 2×10^3 kWh/m^2, although it is less near the equator (but still above 1×10^3 kWh/m^2). Large areas of high storage are found mainly around the Northern and Southern Hemisphere westerlies, and storage gradually decreases towards low latitudes. The distributions of effective storage and exploitable storage of wind energy resources are consistent with total storage.

6. An increasing long-term trend in wind energy was found. For the past 24 years, wind power density has followed a significant increasing trend in most of the global ocean, which should benefit the development of wind energy resource. Areas with a strong increasing trend are mainly located around the Northern Hemisphere westerlies ($>4\ W/m^2$/year) and Southern Hemisphere westerlies ($>8\ W/m^2$/year).
7. In summary, the global ocean is rich in wind energy resource, especially the westerly belts in the Northern and Southern Hemispheres. Indigent areas are mainly found scattered near the equator and poles, while available and subrich areas are located in low latitudes, the coastal waters of the eastern Pacific Ocean at mid to low latitudes, and in most of the polar waters.

Acknowledgments

This work was supported by the National Key Basic Research Development Program Astronomy and Earth Factor on the Impact of Climate Change (Grant no. 2012CB957803), the Special Fund for Public Welfare Industry (Meteorology) (Grant no. GYHY201306026), and the program titled Asian Regional Sea–Air Interaction Mechanism and its Role in Global Change (Grant no. 2010CB950400).

References

[1] Dunnett D, Wallace JS. Electricity generation from wave power in Canada. Renew Energy 2009;34(1):179–95.
[2] Rusu E, Guedes SC. Numerical modeling to estimate the spatial distribution of the wave energy in the Portuguese nearshore. Renew Energy 2009;34(6):1501–16.
[3] Zheng CW, Zhuang H, Li X, Li XQ. Wind energy and wave energy resources assessment in the East China Sea and South China Sea. Science China Technology Science 2012;55(1):163–73.
[4] Zheng CW, Pan J, Li JX. Assessing the China Sea wind energy and wave energy resources from 1988 to 2009. Ocean Eng 2013;65:39–48.
[5] Global Wind Energy Council (GWEC). Global wind energy outlook 2006 report. From 〈http://www.gwec.net〉; 2006.
[6] European Wind Energy Association (EWEA). No Fuel: wind power without fuel, EWEA Campaign. From 〈http://www.no-fuel.org/〉; 2006.
[7] Saidur R, Islam MR, Rahim NA, Solangi KH. A review on global wind energy policy. Renew Sustain Energy Rev 2010;14:1744–62.
[8] Youm I, Sarr J, Sall M, Kane MM. Renewable energy activities in Senegal – a review. Renew Sustain Energy Rev 2000;4:75–89.
[9] Blanco MI. The economics of wind energy. Renew Sustain Energy Rev 2009;13 (6-7):1372–82.
[10] Xiao ZN, Zhu R, Song LL. China wind energy resource assessment. Beijing: China Meteorological Administration Press; 2009.
[11] European Wind Energy Association, EWEA. No Fuel: wind power without fuel, EWEA Campaign. From 〈http://www.no-fuel.org/〉; 2006.
[12] Gaudiosi G. Offshore wind energy in the Mediterranean and other European seas. Renew Energy 1994;5(1):675–91.
[13] Youm I, Sarr J, Sall M, Ndiaye A, Kane MM. Analysis of wind data and wind energy potential along the northern coast of Senegal. Renew Energy 2005;8: 95–108.
[14] Karamanis D. Wind energy resources analysis of Western Greece coast in terms of sustainable environmental indicators and towards their community-based exploitation in South-East Europe. J Renew Sustain Energy 2013;5: 041801, http://dx.doi.org/10.1063/1.4812654.
[15] NASA. Global Ocean Wind energy potential. From 〈http://earthobservatory.nasa.gov/IOTD/view.php?id=8916〉; 2008.
[16] Liu WT, Tang WQ, Xie XS. Wind power distribution over the ocean. Geophys Res Lett 2008;35:L13808, http://dx.doi.org/10.1029/2008GL034172.
[17] Atlas R, Hoffman RN, Ardizzone J, Leidner SM, Jusem JC, Smith DK, Gombos D. A cross-calibrated, multiplatform ocean surface wind velocity product for meteorological and oceanographic applications. Am Meteorol Soc, 92; 2011; 157–74.
[18] Lantz E, Wiseer R, Hand M. IEA Wind task 26: the past and future cost of wind energy. Colorado: National Renewable Energy Laboratory; 2012.
[19] Kozai K, Ohsawa T, Takahashi R, Takeyama Y. Evaluation method for offshore wind energy resources using scatterometer and weibull parameters. J Energy Power Eng 2012;6:1772–8.
[20] Capps SB, Zender CS. Estimated global ocean wind power potential from QuikSCAT observations, accounting for turbine characteristics and siting. J Geophys Res 2010;115:D09101, http://dx.doi.org/10.1029/2009JD012679.
[21] Dong XG, Liu HB, Cao J, Shi ZB, Guo HT, Ma CC. Dynamical downscaling and reserve estimation of wind energy resources in Shandong offshore areas. Resour Sci 2011;33(1):178–83.
[22] Miao WW, Jia HJ, Wang D. Active power regulation of wind power systems through demand response. Sci China Technol Sci 2012;55:1667–76.
[23] Cornett AM. A global wave energy resource assessment. In: Proceedings of the 18th international offshore and polar engineering conference held in Canada; 2008; p. 318–26.
[24] Elliott DL, Holladay CG, Barchet WR, Foote HP, Sandusky WF. Wind energy resource atlas of the United States. DOE/CH 10093-4. Golden, CO, USA: Department of Energy Pacific Northwest Laboratory; 1986.
[25] Wind Energy Resource Atlas of the United States (WERA). the National Renewable Energy Laboratory; 1986. Available from 〈http://rredc.nrel.gov/wind/pubs/atlas〉.
[26] National Development and Reform Commission. Technical requirements for wind energy resource assessment, GB/T 18710-2002. Beijing: Chinese Standard Press; 2004.
[27] Huang SC, Jiang AJ, Liu C, Chen B. Reassessment and study on distribution of wind energy resource in Jiangsu. Sci Meteorol Sinica 2007;27(4):407–12.